Dynamic Adhesion of CD8-positive Cells to Antibody-coated Surfaces: The Initial Step Is Independent of Microfilaments and Intracellular Domains of Cell-binding Molecules

Anne Pierres,* Olivier Tissot,* Bernard Malissen,‡ and Pierre Bongrand*

*Unité INSERM 387, Laboratoire d'Immunologie, Hôpital de Sainte-Marguerite, 13277 Marseille Cedex 09, France; and ‡Centre d'Immunologie de Marseille-Luminy, 13288 Marseille Cedex 09, France

Abstract. Cell adhesion is a multistep, metabolically active process usually requiring several minutes or even hours to complete. This results in the formation of strong bonds that cannot be ruptured by mechanical forces encountered by living cells in their natural environment. However, the first seconds after contact formation are much more sensitive to external conditions and may be the critical step of adhesion. This step is very difficult to monitor without disturbing the observed system.

We addressed this problem by studying the interaction between anti-CD8–coated or control surfaces and murine lymphoid cell lines bearing wild-type CD8 molecules, or genetically engineered molecules bearing extracellular CD8 domains and transmembranar and intracytoplasmic domains of class I histocompatibility molecules, or with extensive deletion of intracytoplasmic domains. We used a new method that consisted of monitoring the motion of cells driven along adhesive surfaces by a hydrodynamic force weaker than the reported strength of single ligand-receptor bonds, but sufficient to make free cells move with an easily detectable velocity of several micrometers per second. Cells exhibited short-term ($\leq$0.5 s) adhesions to the surface with a frequency of about one event per 30-s period of contact. These events did not require specific antigen-antibody bonds. However, when anti-CD8 were present, strong adhesion was achieved within <1 s, since most arrests were longer than a standard observation period of 1 min. This bond strengthening was not affected by cytochalasin, and it did not require intact intracellular domains on binding molecules. It is concluded that the initial step in strong adhesion may be viewed as a passive, diffusion-driven formation of a new specific bonds.

MANY immunological functions, such as T-cell–mediated cytotoxicity, antigen presentation, or T-B cooperation, may be heavily dependent on cellular adhesive interactions. These events may involve a variety of ligand-receptor couples such as LFA-1/intercellular adhesion molecules-1, 2, or 3, CD2/LFA-3, CD4/major histocompatibility complex (MHC)[1] class II, CD8/MHC class I, CD28/B7-BB1, or specific recognition of a MHC-peptide complex by T cell receptors.

The formation of conjugates between cytotoxic T lymphocytes (CTLs) and target cells proved an excellent model to study these interactions. Many experimental findings strongly suggest that the critical step of adhesion is the formation of the first few bonds that will trigger active strengthening, resulting in irreversible attachment. Indeed:

(*a*) Within the very few minutes following contact formation between CTLs and targets, extensive appositions are formed between plasma membranes, with an intercellular gap thinner than several tens of nanometers (and thus compatible with molecular bonding, Springer, 1990) over a contact area of several squared micrometers (Foa et al., 1988).

(*b*) Simultaneously, adhesion molecules are concentrated in the newly formed contact area (Singer, 1976, 1992; André et al., 1990).

(*c*) Numerous studies made in this and other models of T lymphocyte adhesion showed that binding was sensitive to metabolic inhibitors and might require some kind of cell activation (Dustin and Springer, 1989).

(*d*) The mechanical force required to achieve rapid disruption of 50% of conjugates made between L1210 target cells and specific alloimmune murine CTLs was on the order of 100,000 pN (Bongrand and Golstein, 1983). Since the strength of a single ligand-receptor bond is probably <100

Address all correspondence to Pierre Bongrand, Unité INSERM 387, Laboratoire d'Immunologie, Hôpital de Sainte-Marguerite, BP 29, 13277 Marseille Cedex 09, France.

1. *Abbreviations used in this paper*: CTLs, cytotoxic T lymphocytes; MHC, major histocompatibility complex.

pN (Tha et al., 1986; Evans et al., 1991), at least hundreds or thousands of bonds were involved in the interaction. Indeed, the mechanical resistance of cell membranes was the weakest link, since detachment resulted in substantial cell lysis. Interestingly, the mechanical strength of specific interactions between cytotoxic T lymphocytes and target cells displayed time- and temperature-dependent increases after contact formation (Hubbard et al., 1990).

(*e*) In other studies made on the interaction between phagocytes and adhesive surfaces in presence of hydrodynamic flow, it was found that the minimum flow rate required to prevent adhesion was 1,000-fold lower than that required to detach bound cells (Mège et al., 1986, 1990).

It is therefore highly desirable to develop experimental approaches allowing accurate monitoring of the first seconds after the initiation of adhesion. In the present report, we present a possible way of dealing with this problem: cells are driven along adhesive surfaces under continuous microscopic observation and videorecording in a flow chamber operated at extremely low flow velocity. Indeed, if we use a shear rate (see Fig. 1 for definition) of a few seconds^{-1}, it may be shown that the hydrodynamic force experienced by a spherical cell bound to the substrate is about (Goldman et al., 1967):

$$F = 32\ \mu\, a^2\, G,$$

where G is the shear rate (Fig. 1), μ is the medium viscosity, and a is the cell radius. Using a viscosity of 0.0007 Pa × s (corresponding to water and dilute aqueous solutions, Weast et al, 1986) and a cell radius of 4 μm, we obtain:

$$F_{pN} = 0.35\ G_{1/s}.$$

Therefore, the hydrodynamic drag may be considered as much lower than the force exerted by a single bond (Tha et al., 1986; Evans et al., 1991) when the wall shear rate is less than a few tenths of a second^{-1}. Also, the cell inertia is low enough that a force corresponding to a single bond may stop it within a fraction of a second.

As a model system, we studied the interaction between surfaces coated with anti-CD8 monoclonal antibodies and transfected hybridoma cells expressing either wild-type CD8 or mutated CD8 with altered transmembrane and/or intracytoplasmic domains. Results strongly suggest that irreversible adhesion is induced within <1 s, and ligand-cytoskeleton interaction plays no role during this first step of binding. It is shown that an extension of our approach may allow a time resolution of about one tenth of a second.

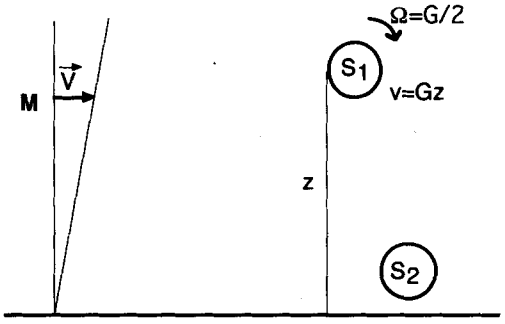

Figure 1. Laminar shear flow near a plane surface. The flow velocity (μm/s) at any point M is parallel to the plane and equal to the product between the shear rate G (s^{-1}) and the distance between M and the plane (μm). A freely flowing sphere at high distance from the plane (*S1*) is expected to display both translation velocity (equal to the unperturbed fluid velocity at the sphere center) and rotation (with angular velocity G/2). When the distance between the sphere and the plane is on the order of the sphere radius or less (*S2*), the translation velocity is substantially lowered with an expected limit of zero when the sphere is in actual contact with the plane (Goldman et al., 1967).

Materials and Methods

Cells

A $CD4^+$ antiovalbumin T cell hybridoma of B10BR origin ($H2^k$; Marrack et al., 1983) was transfected with α and β chain genes encoding T cell receptor of an alloreactive H-$2K^b$–specific cytotoxic T lymphocyte (Letourneur et al., 1990) and (*a*) a CD8α gene, yielding a DC41.1.4 clone; (*b*) a hybrid gene encoding a chimeric polypeptide possessing the extracellular and transmembrane domains of CD8 followed by the last four amino acids from the cytoplasmic domain of the MHC class II A^d gene product, yielding a DC136.2 clone; and (*c*) a hybrid gene encoding a chimeric peptide made of the extracellular domains of CD8 and transmembrane and cytoplasmic domains of class I H-$2K^k$ chain, yielding a DC142.4 clone. A CD8-negative clone (DC183) was used as control. Antigenic and functional properties of transfectants were previously described (Letourneur et al., 1990). Lateral displacements and interactions with the cytoskeleton of transfected CD8 molecules were also studied (André et al., 1991).

Antibodies

Anti-CD8 monoclonal antibody was a rat IgG2b (H35.27.9; Golstein et al., 1982). Another rat IgG2b (H35.17.2, anti-Ly3) and murine anti-CD14 were used as controls, since they did not bind to transfected hybridoma cells.

Flow Chamber

Our apparatus was described in previous reports (Tissot et al., 1991, 1992). Briefly, a rectangular cavity of 17×6×1 mm^3 was cut into a Plexiglas block. The bottom wall of the chamber was a removable glass coverslip (~22×10 mm^2) that was stuck with silicon glue (Rubson, Brussels, Belgium). The flow was generated with a plastic syringe mounted on an electric syringe holder (Razel Scientific Instruments, Stamford, CT, supplied by Bioblock, Illkirch, France) equipped with a 1-rpm or a 2-rpm electric motor. Experiments were performed with cells suspended at 750,000/ml in Hepes-buffered RPMI 1640 medium (Gibco, Glasgow, Scotland) supplemented with 10% fetal calf serum to prevent nonspecific cell-to-glass adhesion. The flow was calibrated as previously described (Tissot et al., 1992; Kaplanski et al., 1993).

Chamber Coating

We used a modification of a method reported by Michl et al. (1979): glass coverslips were washed with ethanol, then incubated with 0.1 mg/ml polylysine hydrobromide (Sigma Immunochemicals, St. Louis, MO; Ref P1524, 680,000 mol wt) for 30 min at room temperature in pH 7.2 phosphate buffer. They were washed and incubated for 60 min in 2.5% glutaraldehyde (Sigma Immunochemicals) in phosphate buffer. They were washed extensively with distilled water and phosphate buffer before another 60-min incubation with 5 μg/ml monoclonal antibodies. They were then rinsed, and unreacted aldehyde groups were blocked by overnight incubation with 0.2 M glycine in 0.1 M phosphate buffer at 4°C. Coverslips were stored in this solution until use.

The surface density was determined by coating glass surfaces with fluorescein-derivatized monoclonals and examining them with a confocal laser scanning microscope (CLSM, Leica, Heidelberg) operated under xz mode. Absolute calibration was achieved by measuring under similar conditions the fluorescence of small volumes (typically 5 μl) of fluoresceinated antibody solutions. Surface coverage was ~410 molecules/μm^2.

Flow Cytometry

1 million cells were incubated for 30 min at 4°C in Eppendorf tubes containing 100 μl of sequential dilutions of monoclonal antibodies. They were then washed twice in 500 μl of RPMI supplemented with 0.1% bovine serum albumin and 10 mM azide. They were incubated another 30 min with fluorescein-derivatized goat anti-mouse antibodies, then washed and assayed with a flow cytometer (Epics Profile; Coulter Corp., Hialeah, FL).

Motion Analysis

The chamber was set on the stage of an inverted fluorescence microscope (Olympus IM; OSI, Paris, France) bearing a X40 Planapo UV objective. The microscope was equipped with a SIT videocamera (model 4015; Lhesa, Cergy Pontoise, France) connected to a digital videotimer (Sopro 600; Soprorep, la Valentine, Marseille, France) allowing time display with 0.1-s accuracy. Images were recorded with a tape recorder (HS338; Mitsubishi Kasei Corp., Tokyo, Japan) for delayed analysis.

In a typical experiment, a single microscope field (215 μm width) was monitored for a fixed period of 5 min, corresponding to the passage of ~50 cells rolling along the chamber floor. Each cell was followed for determination of (*a*) number of detectable arrests (i.e., arrests lasting ≥1 s); and (*b*) number of long-term arrests (i.e., arrests lasting ≥60 s).

A more refined analysis of cell motion was performed as previously described (Kaplanski et al., 1993). Briefly, motion sequences were replayed after connecting the tape recorder to a real time digitizer (PCVision +; Imaging Technology, Bedford, MA) mounted on an AT-type IBM-compatible desk computer. Living images were digitized and displayed on a monitor, which allowed superposition of cell images with a cursor driven by the mouse computer. The motion of individual cells was followed with the mouse and limited images (32×32 pixels, 0.8 μm/pixel) were transferred to the host computer memory typically at a rate of 8 s^{-1}. The cursor position and time were recorded simultaneously with, respectively, one-pixel and 0.01-s accuracy. Images were then examined individually after eightfold enlargement, which allowed rapid determination of cell position with 0.8-μm precision. Positions and times were then stored in a file for delayed analysis of arrests. All operations were performed with software written in the laboratory for this purpose.

Statistical Analysis

Results of individual experiments were pooled to determine the mean frequencies of long- or short-term arrests with the simple formula:

arrest frequency = number of arrests/number of counted cells

The significance of frequency differences observed under variable experimental conditions was calculated as prescribed by Snedecor and Cochran (1980).

Results

It Is Possible to Discriminate between Freely Flowing Cells and Cells Rolling along the Chamber Floor

The determination of binding efficiencies was meaningful only if it was possible to discard cells that were not actually in contact with the adhesive surface. This was easily achieved by combination of several criteria (Fig. 2): (*a*) the microscope was focused on the glass surface so that cells distant from the glass had dim contours. (*b*) The translation velocity of rolling cells was not uniform because of the interaction of surface protrusions with the substrate. (*c*) The trajectory of rolling cells displayed frequent kinks because of interactions with the substrate. (*d*) Finally, the reliability of our criteria was supported by the fact that cells considered as distant from the glass never displayed any detectable arrest. Hence, only cells actually touching the chamber floor were considered in the present study.

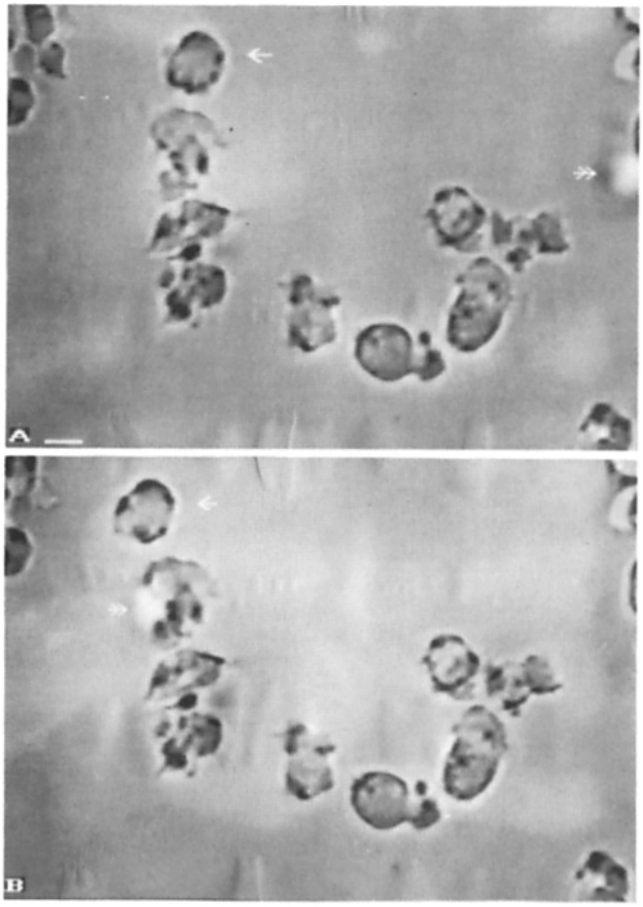

Figure 2. Monitoring cell motion in a flow chamber. Cells were driven along antibody-coated surfaces by a laminar shear flow under continuous video recording. Two frames separated by a time interval of about 1 s are shown (*A* and *B*). Cells remaining in contact with the chamber floor (*arrow*) were easily discriminated from cells flowing at a distance from the wall (*double arrow*). Bar, 6 μm.

Cells Bind to the Substrate through At Least Two Different Mechanisms

The fraction of cells exhibiting at least one detectable stop (i.e., an arrest lasting >~1 s) was measured on anti-CD8-coated surfaces and control coverslips coated with irrelevant antibodies (anti-CD14). As shown in Fig. 3, a substantial proportion of cells displayed binding events, and this was significantly higher when the substrate was coated with specific antibodies. It is thus possible to define specific (CD8-dependent) and nonspecific (CD8-independent) binding mechanisms. As shown in Table I, pretreating lymphoid cells with anti-CD8 antibodies inhibited specific but not nonspecific binding mechanisms, as expected.

Nonspecific Binding Is More Shear-sensitive than Specific Binding

The fraction of detectable stops lasting ≥60 s (heretofore denoted as durable stops) was measured on different substrates and under varying shear rate. As shown in Fig. 4, essentially all arrests were durable in presence of anti-CD8 an-

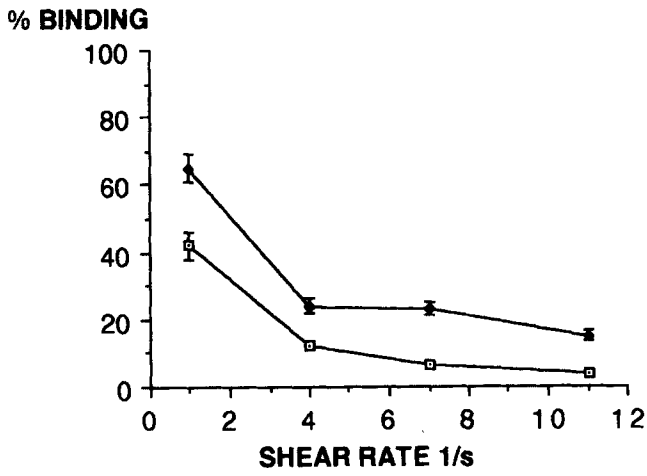

Figure 3. Effect of wall shear rate on cell arrest frequency. Cells expressing CD8 antigen were driven along surfaces bearing anti-CD8 (*black areas*) or irrelevant (*white areas*) antibodies with a wall shear rate ranging between 1 and 11 s^{-1}. The mean number of detectable arrests (≥1 s) per cell was calculated. Each point represents an average value of 153–698 cells. Vertical bar length is twice the standard error. -⊡-, Control; -◆-, anti-CD8.

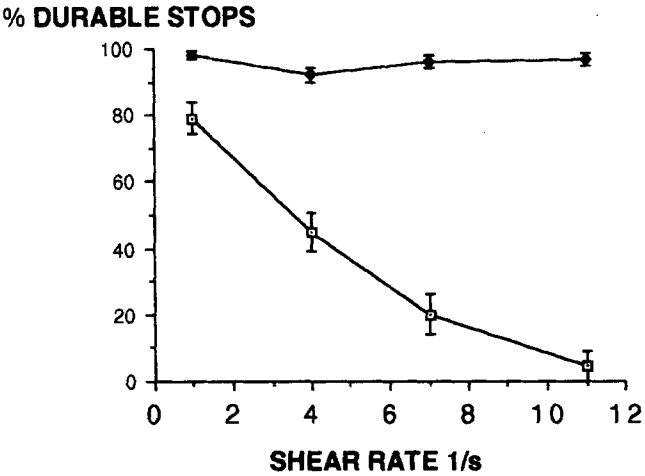

Figure 4. Proportion of durable stops. Cells expressing CD8 antigen were driven along anti-CD8-coated (*black areas*) or control (*white areas*) surfaces by a flow of varying shear rate (abscissa). Detectable cell arrests (>∼1 s duration) were monitored and the proportion of these arrests lasting 60 s or more is shown. Each point represent a population of 153–698 cells. Vertical bar length is twice the standard error. -⊡-, Control; -◆-, anti-CD8.

tibodies, when the shear rate was varied between 1 and 11 s^{-1}. On the contrary, nonspecific arrests were dramatically shortened when the shear rate was increased. Therefore, most stops monitored with a shear rate of ≥4 s^{-1} were caused by specific interactions.

CD8-specific Arrests Do Not Require a Capacity of CD8 Molecules to Interact with Cytoplasmic Cytoskeletal Elements

To assess a possible importance of transmembrane interactions in binding, we compared the adhesive behavior of different clones expressing wild-type, mutated, or truncated CD8 molecules. The surface expression of CD8 was first studied with flow cytometry. Results are shown on Fig. 5. Since all curves displayed similar dependence with respect to antibody concentration, while plateau values differed by a factor of ∼2, it is suggested that clones expressed different numbers of binding sites with similar binding affinity. Adhesion was then studied under flow conditions. As shown in Fig. 6, these clones exhibited fairly variable nonspecific binding ability. As shown in Fig. 7, they displayed essentially similar capacity to form short-term or durable bonds with anti-CD8 antibodies. Noticeably, deletion of intracytoplasmic domains did not impair the cell ability to form nearly 100% durable arrests when the shear rate was varied between 1 and 11 s^{-1}. Further, as shown in Table II, treating cells with cytochalasin B, an inhibitor of microfilament polymerization, did not alter adhesion behavior. Finally, an immediate consequence of the data shown on Figs. 5 and 7 is that there is no correlation between the effectiveness of a CD8 variant in arresting cells and the extent of its expression on the cell

Table I. Effect of Anti-CD8 on Cell Adhesion to Anti-CD8-coated Surfaces

Cell treatment	Chamber coating	Total arrests	Durable arrests
–	Anti-CD8	31% (45/143)	25% (35/143)
Anti-CD8	Anti-CD8	6% (13/209)	6% (12/209)
–	Anti-CD14	13% (15/115)	7% (8/115)
Anti-CD8	Anti-CD14	10% (23/222)	9% (21/222)

Cells expressing CD8 antigen were driven along surfaces coated with anti-CD8 or irrelevant (anti-CD14) antibodies in control medium or in the presence of 5 μg/ml anti-CD8. Wall shear rate was 4 s^{-1}. The percent of cells displaying a detectable (at ≥∼1 s) or durable (≥60 s) arrest is shown together with the number of monitored cells (in parentheses).

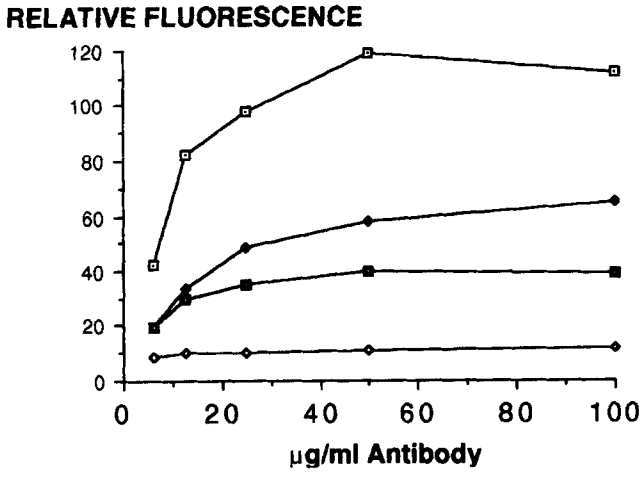

Figure 5. Expression of CD8 by transfected clones. Cells transfected with genes coding for wild-type CD8 alpha chain (DC41.1.4.), deleted (DC136.2), or chimeric (DC142.4) molecules and CD8-negative controls (DC183) were assayed with flow cytometry for expression of CD8 antigen. The relative fluorescence intensity is plotted versus concentration of labeling antibody. -⊡-, DC41.1.4; -◆-, DC142.4; -■-, DC136.2; -◇-, DC183.

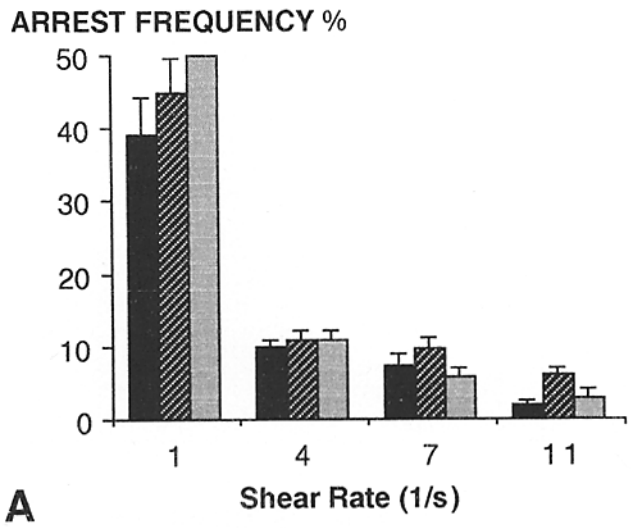

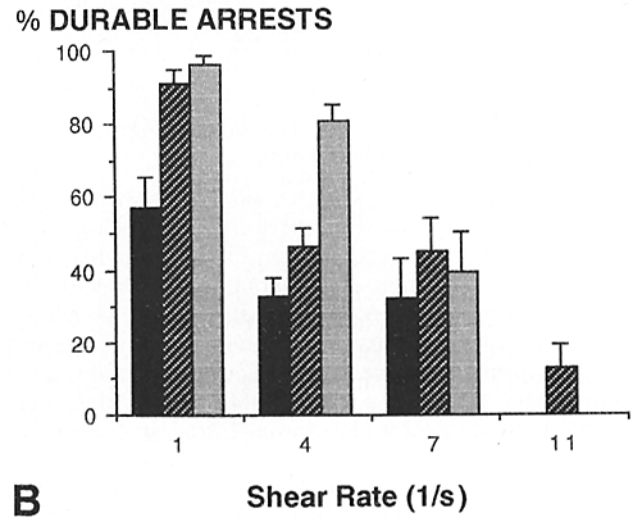

Figure 6. Nonspecific adhesion of lymphocyte clones. Lymphoid cells transfected with wild-type (DC41.1.4), truncated (DC136.2), or chimeric (CD142.4) CD8 were assayed for arrest frequency (>1 s and percent of durable arrests on control surfaces coated with irrelevant (anti-CD14) antibody in presence of a laminar shear flow ranging between 1 and 11 s^{-1}). Vertical bar length is twice the standard error of a cell population ranging between 89 and 919 elements. ■, DC41.1.4; ■ DC136.2; ■ DC142.2.

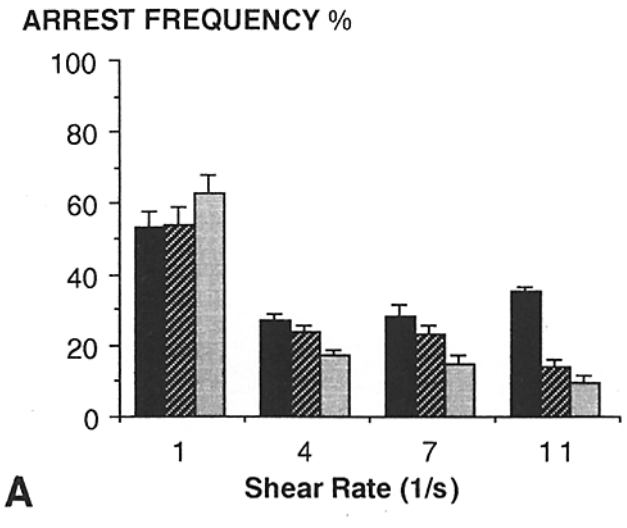

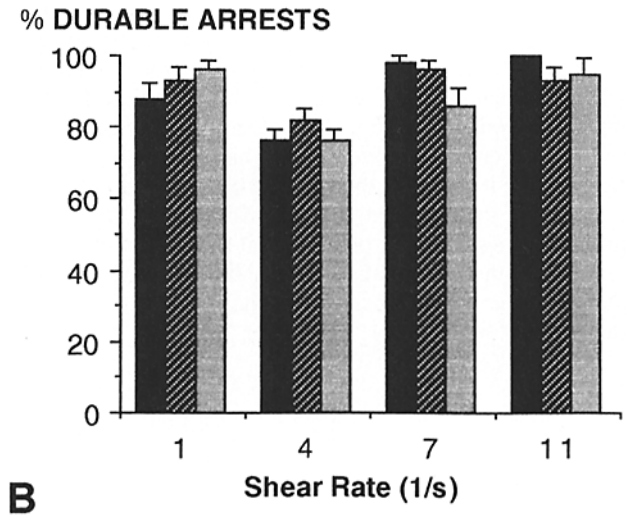

Figure 7. Adhesion of lymphocyte clones to anti-CD8–coated surfaces. Lymphoid cells transfected with wild-type (DC41.1.4), truncated (DC136.2) or chimeric (CD142.4) CD8 were assayed for arrest frequency (≥1 s and percent of durable arrest on control surfaces coated with anti-CD8 antibodies in presence of a laminar shear flow ranging between 1 and 11 s^{-1}). Vertical bar length is twice the standard error of a cell population ranging between 87 and 763 elements. ■, DC41.1.4; ■ DC136.2; ■ DC142.2.

surface. Thus, ligand density may not be a limiting parameter of adhesion.

Specific Adhesion Strengthening Is Inhibited by Cold, not Azide

The influence of either temperature or azide on cell adhesion to anti-CD8–coated surfaces is shown in Table III. Clearly, cold temperature dramatically reduced the duration of cell arrests, whereas cold temperature and azide moderately but significantly reduced the frequency of arrests, whatever their duration.

Table II. Effect of Cytochalasin B on Cell Adhesion to Antibody-coated Surfaces

Cell treatment	Chamber coating	Total arrests	Durable arrests
–	Anti-CD8	22% (104/480)	17% (83/480)
Cytochalasin B	Anti-CD8	25% (95/376)	17% (65/376)

Cells expressing CD8 antigen were driven along surfaces coated with anti-CD8 in control medium or in the presence of 10 μg/ml cytochalasin B. Wall shear rate was 4 s^{-1}. The percent of cells displaying a detectable (≥~1 s) or durable (≥60 s) arrest is shown together with the number of monitored cells (in parentheses).

Table III. Effect of Temperature and Azide on Cell Binding to Antibody-coated Surfaces

Cell treatment	Chamber coating	Total arrests	Durable arrests
–	4°C	13% (44/346)	2% (6/346)
–	25°C	30% (134/447)	22% (98/447)
–	37°C	22% (100/452)	13% (57/452)
Azide	25°C	13% (31/234)	13% (30/234)

Cells expressing CD8 antigen were driven along surfaces coated with anti-CD8 antibodies in control medium or in the presence of 10 mM sodium azide. Temperature was also varied. Wall shear rate was 4 s^{-1}. The percent of cells displaying a detectable ($\geq\sim$1 s) or durable ($\geq$60 s) arrest is shown together with the number of monitored cells (in parentheses).

Adhesion May Be Modeled as a Random Time-dependent Process

A first inspection of Fig. 3 may suggest that cell adhesion is reduced when the relative velocity of cells and substrate is increased. However, it was important to know if the probability of bond formation per unit of time was also decreased when this velocity was increased. To address this question, we measured the mean cell velocity in absence of adhesion when the shear rate was varied. As shown in Fig. 8, a fairly linear relationship was found between the shear rate and cell velocity. Then we replotted the probability for a cell to adhere during its passage through the observation field vs the duration of this passage. As shown in Fig. 9, the binding probability was roughly proportional to the time of observation. This suggested that the probability of bond formation per unit time was independent of the shear rate, when this ranged between 1 and 11 s^{-1}.

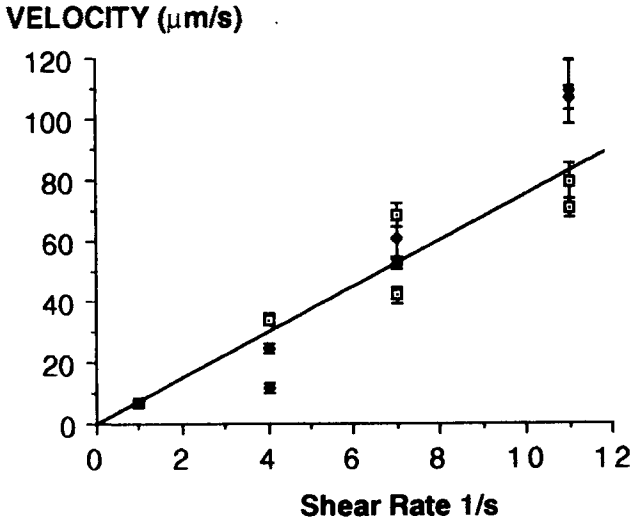

Figure 8. Relationship between shear rate and cell rolling velocity. In 13 independent sets of measurements, the mean velocity of a population of DC41.1.4 cells was determined in presence of a variable shear rate. Only nonadherent cells were studied. Each point represents a mean value determined on a cell population of ~20 elements. Vertical bar length is twice the standard error. ⊡, Control; ♦, anti-CD8.

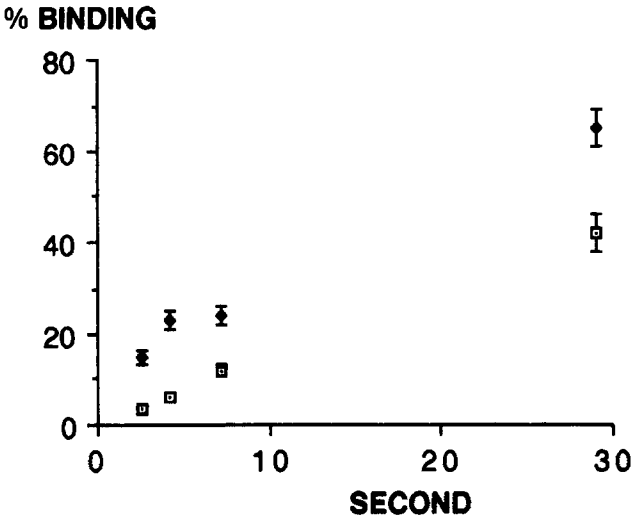

Figure 9. Binding frequency of cells rolling along control or specific antibody-coated surfaces. Data shown on Fig. 4 are displayed by replotting the mean probability that a cell adhered to the substrate during its passage on the microscope field vs the duration of this passage. ⊡, Control; ♦, anti-CD8.

More Refined Analysis Reveals Transient Arrests Lasting a Few Tenths of a Second

We felt it was useful to study transient arrests with higher accuracy. This was achieved by performing individual analysis of sets of digitized cell images (Fig. 10 *A*) suitably enlarged to allow easy measurement of cell position with one-pixel accuracy (Fig. 10 *B*). When cell abscissa was plotted vs time (using 0.12-s steps), as shown in Fig. 11, it appeared that cells displayed frequent slowing events of variable duration, making an objective determination of cell arrests nontrivial. This was obtained by drawing histograms of cell displacements during a given number of time steps. The distributions of displacements of cells driven by a low shear rate (1 s^{-1}) on anti-CD8-coated surfaces is shown in Fig. 12. Clearly, the spatial resolution of one pixel made it impossible to discriminate between arrested and slowly moving cells when a time interval of 0.24 s (two steps) was chosen. However, when higher intervals of 0.72 s (six steps) or 0.96 s (eight steps) were used, the displacement distribution became clearly bimodal, allowing a clear-cut definition of rapidly moving cells (considered as free) and slower elements (considered as substratum/bound). When a higher shear rare (4 s^{-1}) was used, as displayed on Fig. 13, bimodal curves were obtained with a time resolution of 0.24 s. Thus, a cell could be defined as "bound" when it moved by less than three pixels during a time interval of 0.24 s in presence of a flow with a wall shear rate of 4 s^{-1}. This criterium was used to study a population of 67 DC41.1.4 cells flowing on anti-CD8-coated surfaces and 55 cells flowing on control surfaces. The total number of positions recorded were 5542 and 2672, respectively. The mean numbers of arrests (whatever their duration) per cell were 0.69 (46/67) and 0.60 (33/55), respectively. These figures were not significantly different, suggesting that most arrests were mediated by nonspecific interactions. However, when arrest durations were compared (Fig. 14), significant differences were found, since 47% of arrests (22/46) lasted >1 s when surfaces were

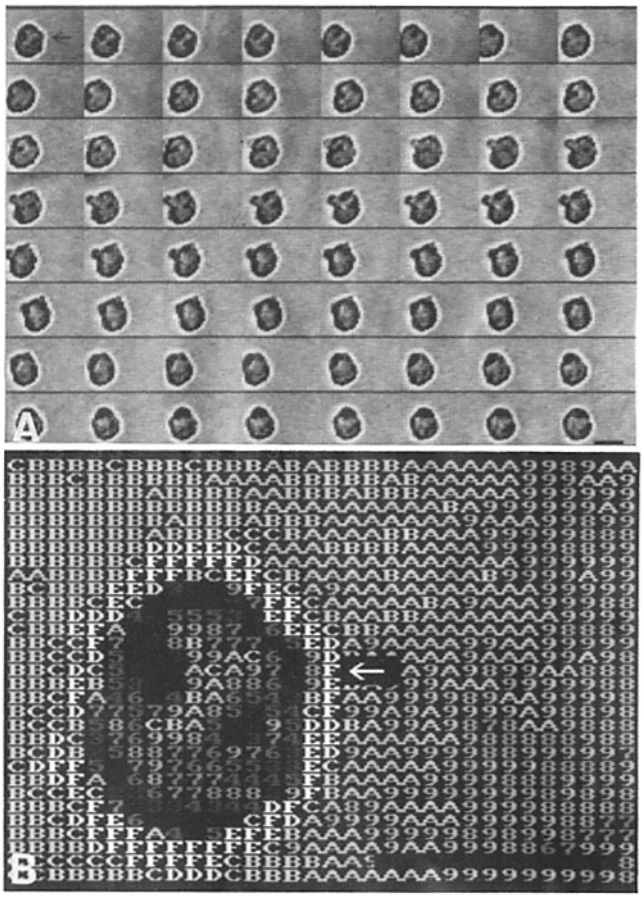

Figure 10. Computer-assisted analysis of cell motion. The images of small fields surrounding a moving cell were sampled every 0.12 s and stored as 64-kilobyte files of 64 images (*A*; bar, 10 μm). The enlarged image of a cell (*arrows*) was used to determine the abscissa of the cell boundary with 1 pixel accuracy (in *B*, individual pixels were displayed as hexadecimal numbers, which allowed immediate reading of the intensity [with 4-bit accuracy]), allowing objective determination of the cell boundary as a local intensity maximum (or minimum, depending on the microscope focusing). Bar, 10 μm.

coated with specific antibodies as compared to 24% (8/33, $P < 0.05$), when only nonspecific interactions were involved. These findings support the view that initial cell arrests were mediated by nonspecific interactions, and bond strengthening was mainly a CD8-dependent event that occurred within ~1 s.

Discussion

A major problem in studying the kinetics of cell adhesion is that it is difficult to demonstrate that a cell is bound to a surface without applying a disturbing force that may alter cell behavior. We tried to overcome this difficulty by subjecting cells to hydrodynamic forces that were at the same time much lower than reported estimates of ligand-receptor bonds (Tha et al., 1986; Evans et al., 1991; Tees et al., 1993) and high enough to make unbound cells move with easily detectable velocity (Fig. 8).

The performance of the method is set by the resolution of cell position measurements (Δx) and the velocity of cells freely rolling on the substratum (v_f). Indeed, an arrest will be detectable if its duration is at least on the order of $\Delta x/v_f$. As shown on Fig. 8, when the wall shear rate ranges between 1 and 10 s^{-1}, v_f is between 6 and 60 μm/s. Since Δx is ~0.8 μm, it should be possible to detect arrests longer than 0.013 s. The video rate of 25–30 frames/s would then be the limiting parameter. Another problem is that arrests become very unfrequent when the wall shear rate is increased (Fig. 3). Thus, it seems reasonable to conclude that in the present study, it was possible to detect cell stops longer than ~0.1–0.2 s, and such events were indeed demonstrated.

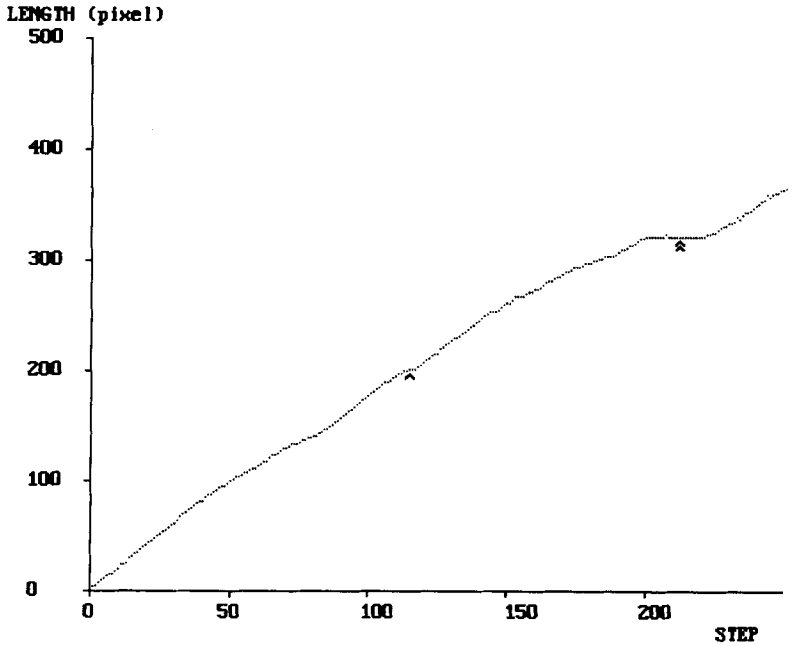

Figure 11. Representation of cell motion. The motion of a typical cell is displayed by plotting cell position (in pixel, ordinate) vs time (in 0.12-s step). Each point represents an individual position, revealing very brief (*arrow*) or longer (*double arrow*) arrests.

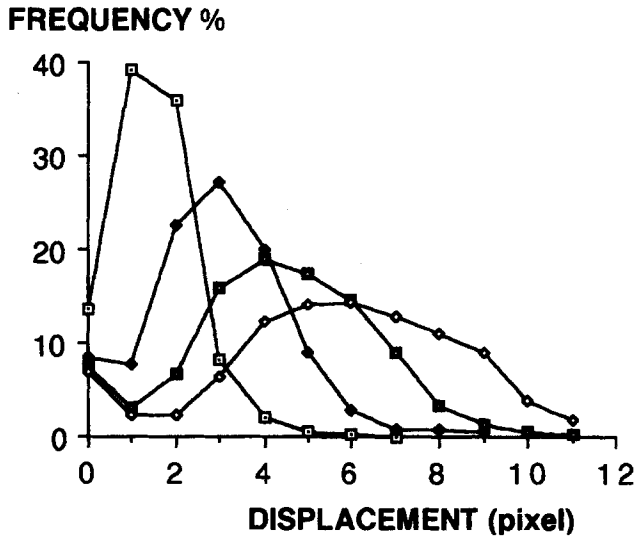

Figure 12. Velocity distribution (low shear rate). The velocity distribution of cells driven along anti-CD8–coated surfaces by an hydrodynamic flow (wall shear rate = 1 s^{-1}) is displayed as a frequency histogram of cell displacements (in pixel) during steps of 0.24, 0.48, 0.72, and 0.96 second. These curves were calculated after observing a total of 4,343 individual displacements of a population of 25 cells. When the time interval is sufficient, curves are bimodal, allowing objective discrimination between so-called "free" and "bound" cells. -□-, 0.24 s; -◆-, 0.48s; -▫-, 0.72 s; -◇-, 0.96 s.

There remains to assess the significance of these cell stops. Three conclusions may be emphasized.

First, as suggested by a qualitative approach (Fig. 4) and supported by a quantitative analysis (Results and Fig. 14), most brief arrests (i.e., arrests shorter than ~0.5 s) were not dependent on specific interactions between CD8 molecules and anti-CD8 antibodies. Clearly, it would be highly desirable to obtain more information on the molecules involved

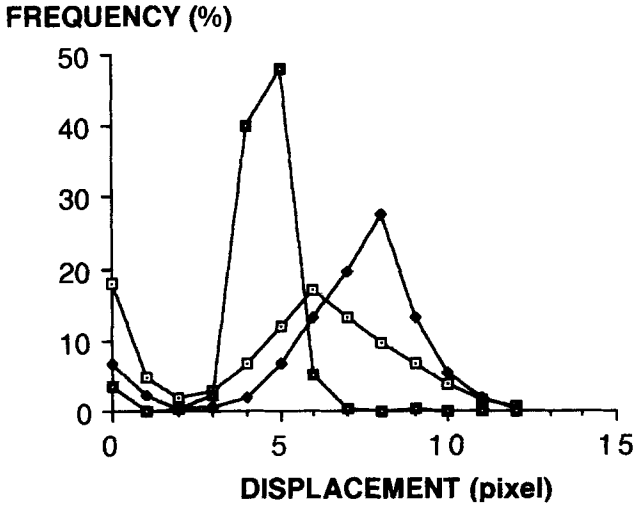

Figure 13. Velocity distribution (medium shear rate). The velocity distribution of cells driven along anti-CD8–coated or control surfaces and spherical beads (8 μm diameter) driven along control surfaces by a flow of 4-s^{-1} wall sheat rate was studied. The frequency histogram of displacements (in pixel) recorded during a time interval of 0.24 s is shown. The curves were calculated with samples of 1125, 1620, and 1897 positions, respectively. All curves exhibit a bimodal pattern, allowing objective discrimination between "free" (i.e., more rapid) and "bound" (i.e., slower) particles. -□-, Anti-CD8; -◆-, control; -▫-, beads.

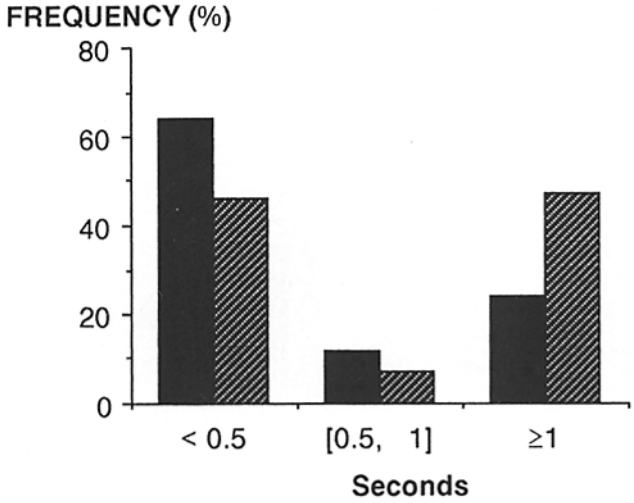

Figure 14. Duration of cell arrests on control or specific antibody-coated surfaces. Cells were driven along control or anti-CD8–coated surfaces with a wall shear rate of 4 s^{-1}. A cell was defined as arrested when it moved by 0 or 1 pixel during a 0.24-s interval (Fig. 13). The distribution of arrest durations was determined on samples of 55 (controls) or 67 (specific antibodies) cells, yielding 33 and 46 arrests, respectively. ■, Control; ▨, anti-CD8.

in the regulation of these short-term binding events. Components of the extracellular matrix may be attractive candidates for such a role.

Second, if it is expected that the lifetime of most nonspecific adhesions do not exceed 0.5 s, in accordance with the data shown in Figure 14, specific antigen-antibody bonds should be involved in the formation of the majority of durable attachments. Interestingly (Fig. 14), most arrests longer than 0.5 s lasted >1 s and often 1 min (Fig. 4). This behavior may be accounted for by a very simple model that was discussed in a previous paper (Kaplanski et al., 1993). The probability that the cell will detach at time t ($P[t]$) may be calculated numerically for different values of the ratio between the rates of formation and dissociation of specific bonds (K^+/K^-). When this ratio is comparable to or higher than unity, $P(t)$ is a sharply decreasing function of time, since either the first bond breaks rapidly or additional bonds are progressively formed, making more and more improbable the simultaneous rupture of all bonds at a later moment. This is in accordance with the view that de-adhesion must be considered as an active process that may involve definite intracellular events (Rees et al., 1977; Marks et al., 1991). Thus, the transient arrests we described might be initiated by the formation of single molecular bonds. Experimental determination of the lifetime of these bonds would require that we decrease the density of binding sites, thus decreasing k^+/k^- so that a substantial fraction of arrested cells would be unable to form multiple bonds. However, this did not seem feasible with the model we used because of the high number of nonspecific adhesions that could not be discriminated from rare specific bonding events. It must be emphasized that this model may be better suited to analyze the present data than the results obtained by Kaplanski et al. (1993). These authors found that anti-E-selectin antibodies decreased the frequency, not the duration, of neutrophil arrests on endothelial cell monolayers. Indeed, as pointed out in their report, molecules other than E-selectin might be involved in adhesion strengthening after cells had stopped.

This is in line with the demonstration by Lawrence and Springer (1991) of a differential role of selectins and integrins in leukocyte-substrate adhesion under conditions of flow. Selectins were most efficient in promoting initial adhesion, but integrins were required for bond strengthening. A different situation was encountered in the present work, since CD8-anti-CD8 interaction was the major mechanism of bond strengthening, whereas nonspecific interactions played a significant role in initial cell arrest.

Third, our results unambiguously support the view that the process of adhesion strengthening that occurs during the seconds after initial attachment is not dependent on active molecular redistributions or deformations of the cell membrane, since it was not decreased by cytochalasin B, and mutated molecules with altered transmembrane and/or cytoplasmic domains displayed similar ability to mediate durable attachment as wild-type molecules. This is consistent with the view that contact triggering of cell deformation (Evans, 1989) or initiation of surface redistribution by receptor cross-linking (as exemplified by the capping phenomenon: Taylor et al., 1971; Bourguignon and Bourguignon, 1984; Kammer et al., 1988; André et al., 1991) usually require several tens or hundreds of seconds to be initiated (even if these processes may be completed within a few seconds when they are triggered). It is therefore likely that the formation of the first few bonds is a passive process that might be described with a biophysical modeling (Hammer and Lauffenburger, 1987), in contrast with a delayed metabolically dependent strengthening that may occur during the minutes or hour after contact formation (McClay et al., 1981). Thus, it may be warranted to use model systems such as spherical beads coated with ligand molecules to study the initial steps of bond formation (Wattenbarger et al., 1990). A potential advantage of this approach would be to allow highly accurate determination of cell position with suitable techniques of image analysis (Uyeda et al., 1991). Since the velocity of such particles under flow conditions may be much more constant than that of actual cells, much briefer arrests should be detectable with our analytical procedure. The overall performance would be also enhanced by making use of specialized video equipment allowing to record several of hundreds of frames per second. This approach is presently in progress in our laboratory.

This work received generous support from the Assistance Publique de Marseille.

Received for publication 8 November 1993 and in revised form 2 February 1994.

References

André, P., A. M. Benoliel, C. Capo, C. Foa, M. Buferne, C. Boyer, A. M. Schmitt-Verhulst, and P. Bongrand. 1990. Use of conjugates made between a cytolytic T cell clone and target cells to study the redistribution of membrane molecules in cell contact areas. *J. Cell Sci.* 97:335–347.

André, P., J. Gabert, A. M. Benoliel, C. Capo, C. Boyer, A. M. Schmitt-Verhulst, B. Malissen, and P. Bongrand. 1991. Wild type and tailless CD8 display similar interaction with microfilaments during capping. *J. Cell Sci.* 100:329–337.

Bongrand, P., and P. Golstein. 1983. Reproducible dissociation of cellular aggregates with a wide range of calibrated shear forces: application to cytolytic lymphocyte-target cell conjugates. *J. Immunol. Methods.* 58:209–224.

Bourguignon, L. Y. W., and G. J. Bourguignon. 1984. Capping and the cytoskeleton. *Int. Rev. Cytol.* 87:195–224.

Dustin, M. L., and T. A. Springer. 1989. T-cell receptor cross-linking transiently stimulates adhesiveness through LFA-1. *Nature (Lond.).* 341: 619–624.

Evans, E. A. 1989. Kinetics of granulocyte phagocytosis: rate limited by cytoplasmic viscosity and constrained by cell size. *Cell Motil Cytoskeleton.* 14:544–551.

Evans, E. A., D. Berk, and A. Leung. 1991. Detachment of agglutinin-bonded red blood cells. I. Forces to rupture molecular-point attachments. *Biophys. J.* 59:838–848.

Foa, C., J. L. Mege, C. Capo, A. M. Benoliel, J. R. Galindo, and P. Bongrand. 1988. T cell-mediated cytolysis: analysis of killer and target cell deformability and deformation during conjugate formation. *J. Cell Sci.* 89:561–573.

Goldman, A. J., R. G. Cox, and H. Brenner. 1967. Slow viscous motion of a sphere parallel to a plane wall. II. Couette flow. *Chem. Eng. Sci.* 22:653–660.

Golstein, P., C. Goridis, A. M. Schmitt-Verhulst, B. Hayot, A. Pierres, A. van Aghtoven, Y. Kaufman, Z. Eshar, and M. Pierres. 1982. Lymphoid cell surface interaction structures detected using cytolysis-inhibiting monoclonal antibodies. *Immunol. Rev.* 68:5–42.

Hammer, D. A., and Lauffenburger, D. A. 1987. A dynamical model for receptor-mediated cell adhesion to surfaces. *Biophys. J.* 52:475–487.

Hubbard, B. B., M. W. Glacken, J. D. Rodgers, and R. R. Rick. 1990. The role of physical forces on cytotoxic T cell target cell conjugate stability. *J. Immunol.* 144:4129–4138.

Kammer, G. E., E. Walter, and M. Medof. 1988. Association of cytoskeletal reorganization with capping of the complement decay accelerating factor on T lymphocytes. *J. Immunol.* 141:2924–2928.

Kaplanski, G., C. Farnarier, O. Tissot, A. Pierres, A. M. Benoliel, M. C. Alessi, S. Kaplanski, and P. Bongrand. 1993. Granulocyte-endothelium initial adhesion. Analysis of transient binding events mediated by E-selectin in a laminar shear flow. *Biophys. J.* 64:1922–1933.

Lawrence, M. B., and Springer, T. A. 1991. Leukocytes roll on a selectin at physiological flow rates: distinction from and prerequisite for adhesion through integrins. *Cell.* 65:859–873.

Letourneur, F, J. Gabert, P. Cosson, D. Blanc, J. Davoust, and B. Malissen. 1990. A signaling role for the cytoplasmic segment of the CD8α chain detected under limiting stimulatory conditions. *Proc. Natl. Acad. Sci. USA.* 87:2339–2343.

Marks, P. W., B. Hendey, and F. R. Maxfield. 1991. Attachment to fibronectin or vitronectin makes human neutrophil migration sensitive to alterations in cytosolic free calcium concentration. *J. Cell Biol.* 112:149–158.

Marrack, P., R. Shimonkewitz, R. Hannun, C. Haskins, and J. Kappler. 1983. The major histocompatibility complex-restricted antigen receptor on T cells. IV. An anti-idiotypic antibody predicts both antigen and I specificity. *J. Exp. Med.* 158:1635–1646.

McClay, D. R., G. M. Wessel, and R. B. Marchase. 1981. Intercellular recognition: quantitation of initial binding events. *Proc. Natl. Acad. Sci. (USA).* 78:4975–4979.

Mège, J. L., C. Capo, P. André, A. M. Benoliel, and P. Bongrand. 1990. Mechanisms of leukocyte adhesion. *Biorheology.* 27:433–444.

Mège, J. L., C. Capo, A. M. Benoliel, and P. Bongrand. 1986. Determination of binding strength and kinetics of binding initiation. A model study made on the adhesive properties of P388D1 macrophage-like cells. *Cell Biophys.* 8:141–160.

Michl, J., M. M. Pieczonka, J. C. Unkeless, and S. C. Silverstein. 1979. Effects of immobilized immune complexes on Fc- and complement-receptor function in resident and thioglycollate-elicited mouse peritoneal macrophages. *J. Exp. Med.* 150:607–621.

Rees, D. A., C. W. Lloyd, and D. Thom. 1977. Control of grip and stick in cell adhesion through lateral relationships of membrane glycoproteins. *Nature (Lond.).* 267:124–128.

Singer, S. J. 1976. The fluid mosaic model of membrane structure: some applications to ligand-receptor and cell-cell interactions. *In* Surface Membrane Receptors. R. A. Bradshaw, W. A. Frazier, R. C. Merrell, D. I. Gottlieb, and R. A. Hogue-Angeletti, editors. Plenum Publishing Corp., New York. pp. 1–24.

Singer, S. J. 1992. Intercellular communication and cell-cell adhesion. *Science (Wash. DC).* 255:1671–1677.

Snedecor, G. W., and W. G. Cochran. 1980. Statistical Methods. Iowa State University Press, Ames, IA 124–128.

Springer, T. A. 1990. Adhesion receptors of the immune system. *Nature (Lond.)* 346:425–434.

Taylor, R. B., W. P. H. Duffus, M. C. Raff, and S. DePetris. 1971. Redistribution and pinocytosis of lymphocyte surface immunoglobulin molecules induced by anti-immunoglobulin antibodies. *Nature New Biol.* 233:225–229.

Tees, D. J., O. Coenen, and H. L. Goldsmith. 1993. Interaction forces between red cells agglutinated by antibody. IV. Time and force dependence of breakup. *Biophys. J.* 65:1318–1334.

Tha, S. P., J. Shuster, and H. L. Goldsmith. 1986. Interaction forces between red cells agglutinated by antibody. II. Measurement of hydrodynamic force of breakup. *Biophys. J.* 50:1117–1126.

Tissot, O., C. Foa, C. Capo, H. Brailly, M. Delaage, and P. Bongrand. 1991. Influence of adhesive bonds and surface rugosity on the interaction between rat thymocytes and flat surfaces under laminar shear flow. Biocolloids and biosurfaces issue. *J. Dispersion Sci. Technol.* 12:145–160.

Tissot, O., A. Pierres, C. Foa, M. Delaage, and P. Bongrand. 1992. Motion of cells sedimenting on a solid surface in a laminar shear flow. *Biophys. J.* 61:204–215.

Uyeda, T. Q. P., H. M. Warrick, S. J. Kron, and J. A. Spudich. 1991. Quantized velocities at low myosin density in an in vitro motility assay. *Nature (Lond.).* 352:307–311.

Wattenbarger, M. R., D. J. Graves, and D. A. Lauffenburger. 1990. Specific adhesion of glycophorin liposomes to a lectin surface in the shear flow. *Biophys. J.* 57:765–777.

Weast, R. C., M. J. Astle, and W. H. Beyer. 1986. CRC Handbook of Chemistry and Physics. 67th ed. CRC Press, Boca Raton, FL. pp. F-37.